ARTICLE

BIOTECHNOLOGY and BIOENGINEERING

Ionic Liquid Activated *Bacillus Subtilis* Lipase A Variants Through Cooperative Surface Substitutions

Jing Zhao,[1] Ning Jia,[1] Karl-Erich Jaeger,[2] Marco Bocola,[1] Ulrich Schwaneberg[1]

[1]Lehrstuhl für Biotechnologie, RWTH Aachen University, Worringerweg 3, 52074 Aachen, Germany; telephone: +49-241-80 24176; fax: +49-241-80 22387; e-mail: u.schwaneberg@biotec.rwth-aachen.de

[2]Institute of Molecular Enzyme Technology, Heinrich-Heine-University Düsseldorf, Forschungszentrum Jülich, 52426 Jülich, Germany

ABSTRACT: The interest in performing enzyme-catalyzed reactions in amphiphilic systems, e.g., imidazolium-based ionic liquids (ILs) or surfactants, has been increased over the past decades. Directed protein evolution has been successful in tailoring enzymes for desired properties. Herein, nine IL-resistant *Bacillus subtilis* lipase A variants, particularly an IL-activated variant M1 (M134N/N138S/L140S), were identified by directed evolution. For instance, variant M2 (M134R/L140S) showed almost doubled specific activity (16.9 vs. 9.4 U/mg) and resistance (233% vs. 111%) at 9 vol% 1-butyl-3-methylimidazolium trifluoromethanesulfonate ($[C_4mim][TfO]$) compared with wild–type. The specific activities and resistance of purified individual single and double variants have been studied in five different IL-aqueous mixtures. The re-activation of lipase variant M1 (not wild–type) at high IL concentration was attributed to the cooperative effect of three surface substitutions (M134N, N138S, L140S) near the substrate-binding cleft. The presence of IL/substrate clusters under assay conditions was likely related to the re-activation effect. This study provides first example of IL-activated lipase variant generated by protein engineering, and helps to better understand the protein-IL interaction.

Biotechnol. Bioeng. 2015;112: 1997–2004.

KEYWORDS: directed evolution; protein engineering; cooperative effects; lipase; ionic liquids; clusters

Introduction

Lipases (EC 3.1.1.3) are a sub-class of enzymes within the esterase family whose natural function is to hydrolyze long chain triacylglycerols (Schmid and Verger, 1998). Lipases constitute an important group of biocatalysts for industrial and biotechnological applications (Anobom et al., 2014; Hasan et al., 2006). Protein engineering has been successful in generating enzyme variants with desired property towards non-natural conditions (Hudson et al., 2005; Liszka et al., 2012; Nordwald and Kaar, 2013). The interest in performing enzyme-catalyzed reactions in non-conventional media such as ionic liquid (IL) has increased in recent years (Bose et al., 2012; Ha et al., 2013; Lehmann et al., 2012; Nordwald et al., 2014; Raddadi et al., 2013; Trivedi et al., 2013; Wolski et al., 2011).

ILs are molten salts composed of organic cations and inorganic or organic anions with melting points typically below 373 K (Freudenmann et al., 2011; Moniruzzaman et al., 2010). Over the past decades, ILs have attracted great attention as possible "green" replacements for conventional organic solvents in chemical and biocatalytic processes due to their unique properties, such as negligible vapor pressure, high thermal stability, good solvation ability and wide electrochemical potential (Earle et al., 2006; Mora-Pale et al., 2011; van Rantwijk and Sheldon, 2007; Zhao, 2010). In addition, ILs can be tuned to specific application demands by changing the anion or/and cation (Giernoth, 2010; Plechkova and Seddon, 2007).

One attractive property of ILs based on 1-alkyl-3-methylimidazolium cation $[C_nmim]^+$ is their inherent amphiphilicity as cationic surfactants depending on the alkyl chain length (Singh and Kumar, 2007; Wang et al., 2007). The aggregation behavior of ILs in aqueous solutions has been reported in many articles (Blesic et al., 2007; Bowers et al., 2004; Mao and Zhu, 2013; Miskolczy et al., 2004; Wang et al., 2007) and reviews (Chen et al., 2014; Greaves and Drummond, 2008; Luczak et al., 2008; Sintra et al., 2014). It is found that the aggregation of ILs is highly dependent on the concentration and type of ILs (e.g., length of alkyl chain and type of anion) (Singh and Kumar, 2007), the buffer system (e.g., salt type and concentration) (Blesic et al., 2007), and other components in the solution (e.g., proteins and reactants used in enzyme-catalyzed reactions) (Ventura et al., 2012). For instance, for a given cation, the ability of anions to promote aggregation of the ILs basically follows the order $I^- > Br^- > Cl^-$, which can be explained by different hydration and binding capacity of them to the cation (Vaghela et al., 2011). In addition, the presence of salts or reactants often significantly decreases the critical aggregation concentrations

Correspondence to: Prof. Dr. Ulrich Schwaneberg
Received 19 February 2015; Revision received 27 March 2015; Accepted 6 April 2015
Accepted manuscript online 20 April 2015;
Article first published online 22 July 2015 in Wiley Online Library (http://onlinelibrary.wiley.com/doi/10.1002/bit.25617/abstract).
DOI 10.1002/bit.25617

(CACs) of the ILs (Blesic et al., 2007; Ventura et al., 2012). Noteworthy, short alkyl chain ILs (n $\leq$4) like [C_4mim]Br and [C_4mim]Cl are hard to form aggregates (Goodchild et al., 2007; Vaghela et al., 2011), nevertheless some studies reported the aggregates of short alkyl chain ILs, e.g., [C_4mim]Cl (Remsing et al., 2008; Singh and Kumar, 2007), [C_4mim][BF_4] (Mao and Zhu, 2013; Singh and Kumar, 2007), [C_4mim][C_8SO_4] (Miskolczy et al., 2004), and [C_4mim][CH_3SO_4] (Modaressi et al., 2007). Additionally, [C_4mim]I clusters have been directly observed for the first time using high-resolution transmission electron microscopy (HRTEM) (Chen et al., 2011). This leaves the question of whether short alkyl chain ILs can form aggregates still open, and the conditions aforementioned should be taken into account.

Since most lipases are activated at the water-lipid interface, their interaction with amphiphilic molecules (e.g., imidazolium-based ILs) is expected to affect their catalytic performance (Goldfeder and Fishman, 2014; Sintra et al., 2014). For instance, Ventura et al. (2012) reported that the activity of the commercial *Candida antarctica* lipase B (CaLB) crude extract could be enhanced up to six fold in aqueous solutions of the long-chain IL 1-decyl-3-methylimidazolium chloride, [C_{10}mim]Cl. This phenomenon was explained by the formation of clusters originated by the self-aggregation of [C_{10}mim]Cl. However, only CaLB wild–type was tested in one IL [C_{10}mim]Cl, thus it is difficult to make general conclusions about the influence of protein-IL interactions on protein activity.

In this study, the *Bacillus subtilis* lipase A (BSLA) (van Pouderoyen et al., 2001) was chosen as a model enzyme with a solved crystal structure (PDB code: 1I6W) and without a "lid" covering the active site. The BSLA wild–type is deactivated at high concentrations of short-alkyl chain imidazolium-based ILs, therefore we performed a directed evolution campaign to identify lipase variants with enhanced IL-resistance. Here, we report the first example of the deactivation of lipase variants at low and re-activation at high IL-concentration. Since this phenomenon is only observed for some specific lipase double or triple variants, the contribution of individual substitutions on cooperative effect is further studied.

Materials And Methods

Chemicals

All chemicals were of analytical grade or higher quality and purchased from Sigma–Aldrich Chemie (Steinheim, Germany), AppliChem (Darmstadt, Germany) and Carl Roth (Karlsruhe, Germany) unless specified. All five ILs ([C_4mim][TfO], [C_2mim][TfO], [C_4mim]Cl, [C_4mim]Br, and [C_4mim]I; Fig. S1) used in this study were purchased from IoLiTec (Ionic Liquid Technologies, Germany) with mass fraction purity higher than 99%. The [C_4mim]Cl and [C_4mim]Br were obtained as solid at room temperature, and were dissolved by adding 8.6% (v/w) and 10% (v/w) Milli-Q water before use.

Plasmids and Strains

The pET22b(+)-*bsla* wild–type plasmid was used as PCR template for construction of random mutagenesis and multiple site saturation mutagenesis libraries. The modified pET22b(+)-*bsla* plasmid harboring an N-terminal His-tag was used as PCR template for site directed mutagenesis. Chemically competent *Escherichia coli* DH5α and *E. coli* BL21-Gold (DE3) cells prepared in-house (3×10^7 and 6×10^5 cfu μg^{-1} pUC19) were used as hosts for DNA manipulation and recombinant protein expression.

Random Mutagenesis

The generation of the random mutagenesis libraries of *bsla* (epPCR with a low- and a high-mutation frequency and SeSaM-Tv P/P) was shown in our previous study (Zhao et al., 2014). The average number of amino acid substitutions per protein for epPCR-low, epPCR-high, and SeSaM-Tv P/P library was 1.1, 4.1 and 1.6, respectively.

Multiple Site Saturation Mutagenesis

Two multiple site saturation mutagenesis (MSSM) libraries, MSSM 138/140 (VDS codon) and MSSM 134/138/140 (MRW codon), were generated using a modified QuikChange protocol (Wang and Malcolm, 1999). The PCR protocol and the used primers (Table S1) are described in supporting information.

Site Directed Mutagenesis

The expression vectors of most improved BSLA variants and their individual single or double variants were constructed using QuikChange site directed mutagenesis. The PCR protocol was modified based on the aforementioned MSSM protocol with some changes: (i) modified pET22b(+)-*bsla* plasmid harboring an N-terminal His-tag was used as PCR template; (ii) annealing temperature of PCR was optimized for each case (55 °C, 60 °C, or 66 °C in most cases). The primers are shown in Table S2.

Activity Assay in 96-well Microtiter Plate

The activity of BSLA lipase in microtiter plate (MTP) was measured based on photometric assay of the released *p*-nitrophenol detected at 410 nm (A_{410}) using a microplate reader, Tecan Infinite M200 Pro (Tecan Group Ltd., Switzerland), and *p*-nitrophenyl butyrate (*p*NPB) was used as substrate. The reaction mixture in MTP per well was prepared by addition of 90 μL of triethanolamine (TEA) buffer (50 mM, pH 7.5) and IL mixture (with varying IL content) to 10 μL of lipase solution (supernatant of culture or 240 ng of purified lipase). The MTP was then incubated at room temperature for 2 h at 900 rpm. Subsequently, 100 μL of the pre-cooled substrate solution (0.5 mM *p*NPB final concentration, 10 vol% acetonitrile and 90 vol % TEA buffer) was added and A_{410} values were measured for 8 min. One unit (U) of enzyme activity was defined as the amount of enzyme releasing 1.0 μmol of *p*-nitrophenol per minute under the assay conditions. The volume fraction used throughout the manuscript corresponds to the IL concentration at which the lipase incubated, and it is reduced to half for the measurement.

Screening Procedure with *p*NPB Assay in 96-well MTP

The mutant libraries were pre-screened for activity on tributyrin LB_{AMP} agar plates. Active transformants which showed halos

surrounding the colonies were picked and grown in LB_{AMP} medium (150 μL per well) in 96-well MTPs. The expression of BSLA in 96-well MTPs is shown in Fig. S2. The supernatant of culture was used for activity assay since BSLA is secreted into the culture when the vector pET22b (+) (harboring pelB-signal sequence) is employed in *E. coli* BL21-Gold (DE3) (Kumar et al., 2014). The resistance of a lipase towards an IL is defined as the ratio of lipase activity in the presence of IL with its activity in the absence of IL. The activities of lipase in the presence and absence of 9 vol% [C_4mim][TfO] (0.4 M; leading to 31% of resistance for BSLA wild–type; Fig. S3) were measured as previously described. To calculate the activity of the BSLA lipase, the background activity (supernatant of culture with empty vector) was subtracted. The standard deviation of the 96-well MTP-based *p*NPB screening system was determined using supernatant of culture with BSLA wild–type (Fig. S4). Only BSLA variants with increased resistance and clear activity were chosen as the candidates. All the candidates were rescreened in triplicate to identify the improved variants.

Expression of BSLA in Flask and Purification

The main expression culture in flask (containing a modified auto-induction medium) was cultivated at 37°C (250 rpm) for 3 h. Afterwards the temperature was shifted to 15°C for 72 h. The cells were then harvested by centrifugation (4°C, 4000 g, 20 min), and stored at −20°C. The cell pellets were resuspended in lysis buffer (pH 8.0; 50 mM NaH_2PO_4 and 300 mM NaCl) prior to disruption by sonication. The His-tagged BSLA wild–type and variants were purified using the Protino® Ni-TED 2,000 packed columns (Macherey-Nagel). Afterwards, PD-10 desalting column (GE Healthcare, Germany) was used to remove the salts. The purified lipases were stored at glycine buffer (10 mM, pH 10.5) in small aliquots at −20°C, and each aliquot was used only once after thawing. Purity was determined using the Experion™ system from Bio-Rad (München, Germany).

Electrical Conductivity Measurements

The conductivity of the sample was measured using a Seven Compact™ S230 (Mettler Toledo Instruments) at 298 K. At least three measurements were performed for each concentration of IL-aqueous mixture.

Dynamic Light Scattering

Dynamic light scattering (DLS) was employed to determine the presence as well as size of aggregates formed in the IL-aqueous mixtures using a Nano-ZS, ZetaSizer from Malvern Instruments. The particle size detection range of this Nano-ZS Instrument is specified by Malvern Instruments with 0.3 nm to 10.0 μm. All sample solutions were passed through 0.22 μm PVDF membrane filters to remove dust. To ensure adequate mixing, the IL-aqueous mixtures were mixed on a vortex mixer, and incubated at 900 rpm for 2 h. Experiments were performed at 25 °C, and three measurements were taken for each solution. Samples were equilibrated for 10 min before data collection.

Molecular Dynamics Simulations

The molecular dynamics (MD) simulations of [C_4mim]I aqueous mixtures were performed with Amber03 and GAFF force field using YASARA software (Duan et al., 2003; Krieger et al., 2002). The partial charge of $[C_4mim]^+$ was computed using HF/6-31G*-RESP. Electrostatics was calculated using a cutoff of 7.86 Å; long-range interactions were calculated by using the particle-mesh Ewald integration. MD simulations were carried out at 298 K for 30 ns.

Results And Discussion

Directed BSLA Evolution for Improved Resistance Towards 9 vol% [C_4mim][TfO]

First, two rounds of random mutagenesis campaigns have been performed to improve BSLA resistance towards an IL-aqueous solution, nine vol% [C_4mim][TfO] (Fig. 1). Three different random mutagenesis strategies (epPCR-low, epPCR-high, and SeSaM-Tv P/P) were employed in the first round of evolution. Consequently, four improved BSLA variants exhibiting 1.3–1.9 fold increase in resistance to IL were identified after screening of ∼3000 clones in MTP plates. Notably, three of these four improved variants were screened from the SeSaM-Tv P/P library (Fig. 1 and Table S3) which has been previously reported to be enriched in transversions and consecutive nucleotide mutations (Zhao et al., 2014). One variant F58Y/L140S was identified from the epPCR-high library. These four improved variants were selected as parents for the second round of directed evolution using epPCR with a high-mutation frequency (Fig. 1 and Table S3). As a result, a variant V74I/M134K/N138R/G175D with 1.9-fold increased resistance was identified from the second round of directed evolution (Fig. 1).

The locations of all observed amino acid substitutions in the improved variants were mapped on the BSLA structure, and three structurally-related positions (M134, N138, and L140) were finally identified as "hot-spots" (Fig. 2). We observed that N138 and L140 are located on a small helix at the entrance of the substrate-binding cleft (Fig. 2B), while M134 is found on the connecting loop region and adjacent to the active site residue D133. Next, two MSSM libraries, MSSM 138/140 and MSSM 134/138/140, were generated and screened for the improved resistance towards 9 vol% [C_4mim][TfO]. After screening ∼1000 clones of each library, the two most improved variants (M1: M134N/N138S/L140S; M2: M134R/L140S) (Table S3) were selected for further analysis.

Specific Activities and Resistance of Purified BSLA Variants in Five IL-Aqueous Solutions

The variants M1, M2 and their individual single and double variants (Fig. 1) were purified in preparation for characterization (Fig. S5). Initially, two important issues needed to be addressed: (i) in order to maintain the pH of the IL aqueous solutions after reaction: 100 mM TEA buffer (pH 7.5) was selected to control pH shift less than 0.2; (ii) since IL itself can hydrolyze the substrate *p*NPB, the activities of the purified lipases were normalized by subtracting the autohydrolysis rate.

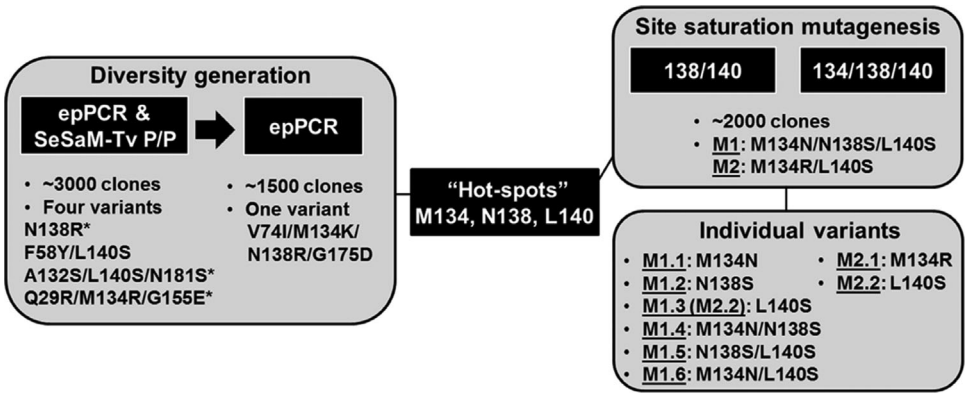

Figure 1. Overview of the directed BSLA evolution campaign. Two iterative cycles of random mutagenesis were performed yielding several improved variants. Asterisks indicate the improved variants screened from SeSaM-Tv P/P library (see details in Table S3). Three structurally-related "hot-spots" (M134, N138, and L140) were identified. Two multiple site saturation mutagenesis (MSSM) libraries, MSSM 138/140 (VDS codon) and MSSM 134/138/140 (MRW codon), were generated and screened.

The specific activities and resistance of purified BSLA wild–type and variants were examined in five ILs, [C_4mim][TfO], [C_2mim][TfO], [C_4mim]Cl, [C_4mim]Br, and [C_4mim]I (Fig. S1). A typical "bell-shaped" resistance curve was observed for BSLA wild–type in all [C_4mim]-based ILs, and similar profiles were reported (Akbari et al., 2011; Daneshjoo et al., 2011; Yang et al., 2010) in other enzyme/IL systems. As expected, the purified M1 and M2 showed enhanced resistance compared to wild–type in almost all studied [C_4mim][TfO] concentrations (Fig. S6), e.g., M2 showed almost doubled specific activity (16.9 vs. 9.4 U/mg) and resistance (233% vs. 111%) at 9 vol% [C_4mim][TfO] than that of purified wild–type. However, lower resistance were found for M1 and M2 in all studied [C_4mim]Cl and [C_4mim]Br concentrations (Figs. S8 and S9). This demonstrated that the property of BSLA was highly dependent on the types of ILs and amino acid substitutions. The specific activities and resistance of identified IL tolerant/activated variants are summarized in Table I. We focus on the discussion of [C_4mim]I in the following paragraph.

Figure 3 shows the specific activities of purified BSLA wild–type and selected variants at 0, 18, and 22 vol% [C_4mim]I solutions (see details in Fig. 4 and Fig. S10). As expected, the specific activity of wild–type was reduced from 10.9 in 0 vol% (buffer) to 6.0 and 4.1 U/mg at 18 vol% and 22 vol% [C_4mim]I, respectively. Surprisingly, an unusual activity profile was observed in the case of M1; within a wide range of low [C_4mim]I concentrations (5–18 vol%), the specific activity of M1 was almost completely lost, however, at 20–22 vol% the activity was dramatically regained (up to ~1.3-fold; 5.9 U/mg compared to 4.6 U/mg in buffer; Fig. S10). These experimental results clearly demonstrated that M1, but not wild–type was reactivated at elevated concentrations of [C_4mim]I (>18 vol%) (Fig. 4). Analyzing the specific activities of individual single variants indicated that M1.2 (N138S) and M1.3 (L140S) were only slightly activated at concentrations above 20 vol% and 18 vol% [C_4mim]I; no "clear" activation was found for M1.1 (M134N). Furthermore, all three double variants (M1.4: M134N/N138S; M1.5: N138S/L140S and M1.6: M134N/L140S) showed only a weak

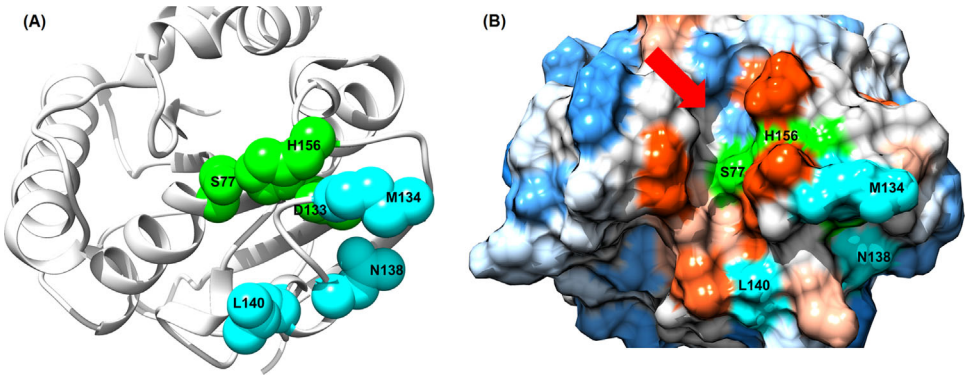

Figure 2. Locations of structurally-related "hot-spots" highlighted on the crystal structure of BSLA (PDB code: 1I6W). (**A**) Three catalytic residues (S77, D133 and H156) are shown in green spheres, and three substitutions (M134, N138, and L140) in cyan spheres. (B) The BSLA surface is colored from hydrophobic (orange) to hydrophilic (blue). The substrate-binding cleft is indicated by the red arrow.

Table I. Summary of the identified ionic liquid tolerant/activated BSLA variants.

Variant	Substitution	Ionic liquid aqueous solution[a]	Specific activity (U/mg)	Resistance relative to WT (%)
Wild-type	—	[C_4mim][TfO]	9.4 ± 0.2	100 ± 6
		[C_2mim][TfO]	5.4 ± 0.3	100 ± 10
		[C_4mim]Cl	22.1 ± 1.0	100 ± 11
		[C_4mim]Br	15.4 ± 1.0	100 ± 13
		[C_4mim]I	4.1 ± 0.3	100 ± 11
M1	M134N/N138S/L140S	[C_4mim][TfO]	8.9 ± 0.4	190 ± 18
		[C_4mim]I	5.9 ± 0.4	340 ± 42
M1.1	M134N	[C_2mim][TfO]	4.5 ± 0.2	200 ± 12
		[C_4mim]Cl	17.3 ± 0.7	170 ± 20
		[C_4mim]Br	11.3 ± 0.2	160 ± 18
M1.2	N138S	[C_2mim][TfO]	5.1 ± 0.5	230 ± 28
M1.3	L140S	[C_4mim][TfO]	13.0 ± 0.4	200 ± 14
		[C_2mim][TfO]	8.3 ± 0.3	270 ± 19
M1.4	M134N/N138S	[C_4mim][TfO]	9.5 ± 0.3	200 ± 15
M1.5	N138S/L140S	[C_4mim][TfO]	11.2 ± 0.3	160 ± 10
M1.6	M134N/L140S	[C_4mim][TfO]	11.6 ± 0.2	240 ± 11
		[C_2mim][TfO]	5.8 ± 0.3	720 ± 64
		[C_4mim]I	4.3 ± 0.3	350 ± 47
M2	M134R/L140S	[C_4mim][TfO]	16.9 ± 0.7	210 ± 19
		[C_2mim][TfO]	10.5 ± 0.2	340 ± 24

[a]The concentration of [C_4mim][TfO], [C_2mim][TfO], [C_4mim]Cl, [C_4mim]Br, [C_4mim]I aqueous solution is 9 vol%, 22 vol%, 30 vol%, 30 vol%, and 22 vol%, respectively.

activation effect and M1.6 was not "fully" deactivated at low [C_4mim]I concentrations. Interestingly, although single variant M1.1 (M134N) behaved similar to wild–type, this amino acid substitution could strengthen the deactivation at low (<18 vol%) and re-activation at high [C_4mim]I concentrations (>18 vol%) of M1.5 (N138S/L140S) when combining these three substitutions (M1: M134N/N138S/L140S). Consequently, the triple variant M1 showed the most significant deactivation at low (<18 vol%) and re-activation at high [C_4mim]I concentrations (>18 vol%), suggesting cooperative effects between the three substitutions (M134N, N138S and L140S). A 3.4-fold increase in resistance was found for M1 at 22 vol% [C_4mim]I compared to wild–type.

Explanation for "Re-Activation Effect"

As mentioned, the imidazolium-based ILs (also the short-chain ILs) may form clusters at high concentrations. In order to evaluate whether the observed activation was related to the clusters of [C_4mim]I, electrical conductivity measurements, DLS and MD simulation study were performed.

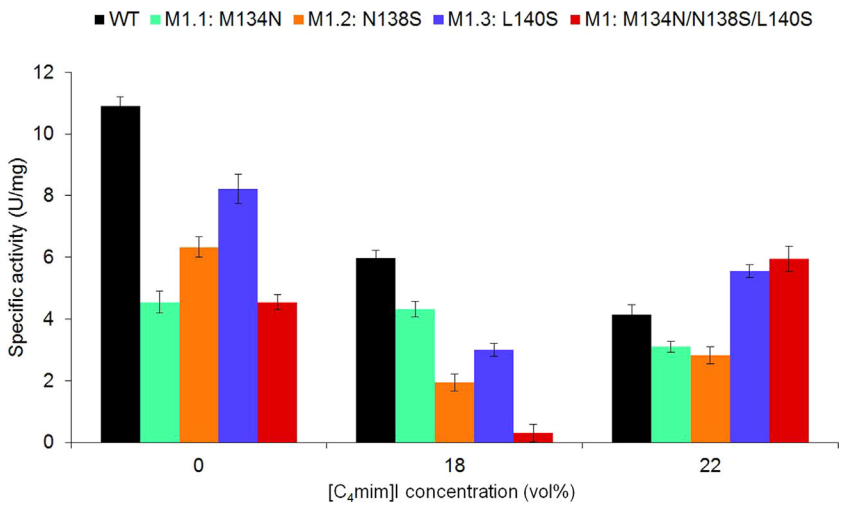

Figure 3. Specific activities of purified BSLA wild–type and selected variants in varied concentration of [C_4mim]I. All values reported are the average of four experimental replicates and deviations are calculated from the corresponding mean values. CAC (critical aggregation concentration) of [C_4mim]I under assay conditions was determined to be ~16 vol%. See details in Fig. S10.

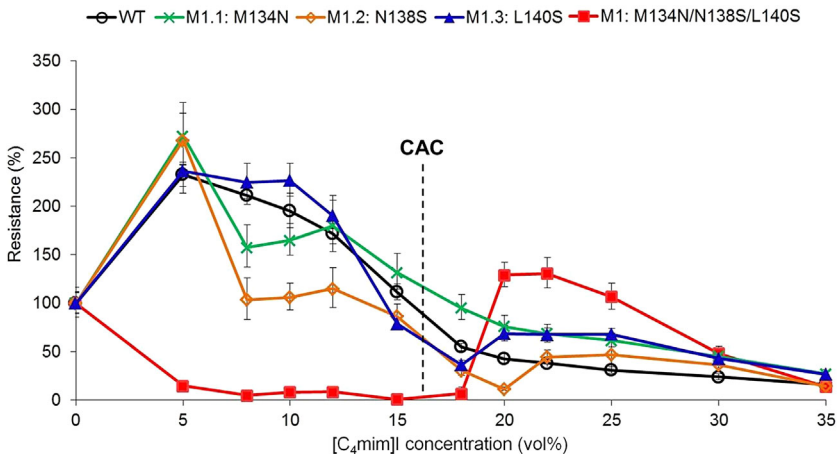

Figure 4. Resistance of purified BSLA wild-type and selected variants in varied concentration of [C_4mim]I. The CAC of [C_4mim]I is ~16 vol%. All values reported are the average of four experimental replicates and deviations are calculated from the corresponding mean values.

The CAC of [C_4mim]I under assay condition (in the presence of substrate *p*NPB) was determined by conductivity measurements. As a result, the CAC was estimated to be ~16 vol% (433 mM, Fig. S11). Activation of M1 at IL concentrations >18 vol% suggested that the activation might be related to the presence of clusters of [C_4mim]I and the substrate under assay conditions.

To confirm the formation of [C_4mim]I clusters, DLS measurements were performed to determine the presence as well as size of clusters. It was found that, clusters in the 0.6–2.0 nm size range were only dominantly present at higher [C_4mim]I concentrations (e.g., 22 and 30 vol%) which are above the CAC (~16 vol%) (Fig. S12). The size of [C_4mim]I clusters was in good agreement with values from literature (0.9–3 nm as reported for other ILs) (Ventura et al., 2012; Wang et al., 2008).

MD simulations were performed to study the [C_4mim]I behavior at [C_4mim]I concentrations below (5 vol%) and above CAC (25 vol %). At 5 vol% of [C_4mim]I, the $[C_4mim]^+$ cations were distributed over the simulation box in monomeric form, and no formation of clusters were observed. However, $[C_4mim]^+$ ions tend to form clusters at 25 vol% [C_4mim]I, and one example of $[C_4mim]^+$ clusters is shown in Fig. S13.

We demonstrated that the observed lipase activation by higher concentration of [C_4mim]I (>18 vol%) may be related to the formation of [C_4mim]I clusters under assay conditions. The clear re-activation effect above CAC only occurred with [C_4mim]I, but not for [C_4mim]Br and [C_4mim]Cl, which could be explained by the fact that [C_4mim]I is more polarizable and has much lower CAC (433 vs. 706 and 728 mM for [C_4mim]Br and [C_4mim]Cl, respectively; Fig. S11), and the significant higher percentage of clusters in the ~0.9 nm size range (97% for 30 vol% [C_4mim]I vs. only 36% and 30% for 40 vol% [C_4mim]Br and 40 vol% [C_4mim]Cl, respectively; Fig. S12). Since CaLB can be activated by high concentration of [C_{10}mim]Cl (Ventura et al., 2012), we also tested purified CaLB in varied content of [C_4mim]I. It was found that CaLB behaved similar to BSLA wild–type, and only inhibition was observed (Fig. S14). This might be due to a very hydrophobic and narrow substrate–binding channel (10 Å × 4 Å) in the wild–type of CaLB (Fig. S15) (Uppenberg et al., 1994), which results in easier access of $[C_4mim]^+$ monomers than *p*NPB/$[C_4mim]^+$ clusters, leading to inhibition (Fig. S14) and not activation.

One interesting question is why the lipase activation was only observed for some specific variants (e.g., M1), but not for wild–type, since [C_4mim]I clusters should be formed in both cases. Previous work (Dwars et al., 2005; Guha and Jaffe, 1996) showed that hydrophobic compounds preferentially partition into the micellar phase, resulting in higher substrate concentration in the vicinity of clusters. Thus, the activity is expected to be enhanced if the lipase substrate-binding site preferentially interacts with mixed substrate/IL clusters. Since BSLA contains no "lid" and its hydrophobic substrate-binding cleft is pre-formed, the substitutions M134N, N138S, and L140S could directly affect the polarity and size/shape of the substrate-binding cleft. Fig. S16 shows a model of variant M1 interacting with the *p*NPB/$[C_4mim]^+$ clusters. It suggests that the substitutions M134N, N138S, and L140S result in a larger and more polar substrate-binding cleft environment, allowing better accommodation of the mixed *p*NPB/$[C_4mim]^+$ clusters and thus promote substrate access. The cooperative effect of three substitutions (M134N, N138S, and L140S) might result in higher residence probability of $[C_4mim]^+$ cations close to the substrate-binding cleft, yielding inhibition at medium [C_4mim]I concentrations (< CAC; cleft blocked by monomeric $[C_4mim]^+$ cations; Fig. S17A) and activation at higher [C_4mim]I concentrations (>CAC; Fig. S17B) forming substrate/IL clusters. Although at concentrations above CAC, a small portion of $[C_4mim]^+$ should still exist in free monomers, variant M1 prefers to contact with *p*NPB/$[C_4mim]^+$ clusters (activation occurs) than $[C_4mim]^+$ monomers (inhibition) because lipase M1 may preferentially bind towards the large interface between water and IL/substrate cluster (Ventura et al., 2012) through cooperative effects within the area containing three substitutions (M134N, N138S, and L140S)

next to the active site entrance. This can be compared to the interfacial activation of typical lipases (due to formation of substrate clusters/micelles) and their preference towards hydrophobic interfaces (Reis et al., 2009; Stamatis et al., 1999). A comparison of the hydrophobicity of BSLA wild–type, M1 and CalB is shown in Fig. S15. At increased $[C_4mim]I$ concentrations above 22 vol%, the specific activity of M1 was gradually reduced likely due to (i) average size of clusters may become bigger (Fig. S12) (Goodchild et al., 2007), leading to less access of *p*NPB/$[C_4mim]^+$ clusters to substrate-binding cleft, and in turn more $[C_4mim]^+$ monomers may block the active site; (ii) fewer substrate molecules are present per cluster at very high IL concentrations; (iii) lower water activity and higher viscosity of the reaction mixture may limit the diffusion of substrates and products (Lou et al., 2006). Thus, the loop area near the active site seems to play a crucial role on the lipase-IL interactions and promotes surface contacts with polar IL-clusters containing a large and polarizable anion like iodide.

Conclusions

In conclusion, here we report one IL-activated and several IL-tolerant BSLA variants which were generated by directed protein evolution. The lipase re-activation above CAC of $[C_4mim]I$ was attributed to a cooperative effect of three surface substitutions near the active site at molecular level, and was likely related to the presence of IL/substrate clusters. This study reveals first insights into the interaction of a lipase active site with ILs, and gains a better understanding of lipase behavior in ILs or surfactants. This provides a general strategy to improve lipases and other enzymes by surface engineering near the active site.

We are grateful for financial support from the DFG research training group 1166 Biocatalysis using non-conventional media (BioNoCo), China Scholarship Council (CSC) scholarship (No. 2011674003) and Chinese Academy of Sciences Visiting Professorships for Senior International Scientists (Y3J8041101) to Prof. Ulrich Schwaneberg. The purified *Candida antarctica* lipase B (CaLB) was kindly supplied by Heidi Höck (RWTH Aachen University). The expression and activity assay procedures of BSLA in 96-well MTPs were supplied by Victorine Josiane Frauenkron–Machedjou (RWTH Aachen University). We thank Dr. Tsvetan Kardashliev and Dr. Mehdi D. Davari (RWTH Aachen University) for critical reading of the manuscript and fruitful discussions.

References

Akbari N, Daneshjoo S, Akbari J, Khajeh K. 2011. Isolation, Characterization, and Catalytic Properties of a Novel Lipase Which Is Activated in Ionic Liquids and Organic Solvents. Appl Biochem Biotechnol 165(3-4):785–794.

Anobom CD, Pinheiro AS, De-Andrade RA, Aguieiras ECG, Andrade GC, Moura MV, Almeida RV, Freire DM. 2014. From Structure to Catalysis: Recent Developments in the Biotechnological Applications of Lipases. Biomed Res Int Article ID 684506, 11 pages, doi:10.1155/2014/684506

Blesic M, Marques MH, Plechkova NV, Seddon KR, Rebelo LPN, Lopes A. 2007. Self-aggregation of ionic liquids: Micelle formation in aqueous solution. Green Chem 9(5):481–490.

Bose S, Barnes CA, Petrich JW. 2012. Enhanced stability and activity of cellulase in an ionic liquid and the effect of pretreatment on cellulose hydrolysis. Biotechnol Bioeng 109(2):434–443.

Bowers J, Butts CP, Martin PJ, Vergara-Gutierrez MC, Heenan RK. 2004. Aggregation behavior of aqueous solutions of ionic liquids. Langmuir 20(6):2191–2198.

Chen S, Kobayashi K, Kitaura R, Miyata Y, Shinohara H. 2011. Direct HRTEM Observation of Ultrathin Freestanding Ionic Liquid Film on Carbon Nanotube Grid. ACS Nano 5(6):4902–4908.

Chen S, Zhang S, Liu X, Wang J, Wang J, Dong K, Sun J, Xu B. 2014. Ionic liquid clusters: structure, formation mechanism, and effect on the behavior of ionic liquids. Phys Chem Chem Phys 16(13):5893–5906.

Daneshjoo S, Akbari N, Sepahi AA, Ranjbar B, Khavarinejad RA, Khajeh K. 2011. Imidazolium chloride-based ionic liquid-assisted improvement of lipase activity in organic solvents. Eng Life Sci 11(3):259–263.

Duan Y, Wu C, Chowdhury S, Lee MC, Xiong G, Zhang W, Yang R, Cieplak P, Luo R, Lee T. Others. 2003. A point-charge force field for molecular mechanics simulations of proteins based on condensed-phase quantum mechanical calculations. J Comput Chem 24(16):1999–2012.

Dwars T, Paetzold E, Oehme G. 2005. Reactions in micellar systems. Angew Chem Int Ed Engl 44(44):7174–7199.

Earle MJ, Esperanca JMSS, Gilea MA, Lopes JNC, Rebelo LPN, Magee JW, Seddon KR, Widegren JA. 2006. The distillation and volatility of ionic liquids. Nature 439(7078):831–834.

Freudenmann D, Wolf S, Wolff M, Feldmann C. 2011. Ionic liquids: New perspectives for inorganic synthesis?. Angew Chem Int Ed Engl 50(47):11050–11060.

Giernoth R. 2010. Task-specific ionic liquids. Angew Chem Int Ed Engl 49(16):2834–2839.

Goldfeder M, Fishman A. 2014. Modulating enzyme activity using ionic liquids or surfactants. Appl Microbiol Biotechnol 98(2):545–554.

Goodchild I, Collier L, Millar SL, Prokes I, Lord JCD, Butts CP, Bowers J, Webster JRP, Heenan RK. 2007. Structural studies of the phase, aggregation and surface behaviour of 1-alkyl-3-methylimidazolium halide plus water mixtures. J Colloid Interface Sci 307(2):455–468.

Greaves TL, Drummond CJ. 2008. Ionic liquids as amphiphile self-assembly media. Chem Soc Rev 37(8):1709–1726.

Guha S, Jaffe PR. 1996. Bioavailability of hydrophobic compounds partitioned into the micellar phase of nonionic surfactants. Environ Sci Technol 30(4):1382–1391.

Ha SH, Anh TV, Koo YM. 2013. Optimization of lipase-catalyzed synthesis of caffeic acid phenethyl ester in ionic liquids by response surface methodology. Bioprocess Biosyst Eng 36(6):799–807.

Hasan F, Shah AA, Hameed A. 2006. Industrial applications of microbial lipases. Enzyme a Micro Technol 39(2):235–251.

Hudson EP, Eppler RK, Clark DS. 2005. Biocatalysis in semi-aqueous and nearly anhydrous conditions. Curr Opin Biotechnol 16(6):637–643.

Krieger E, Koraimann G, Vriend G. 2002. Increasing the precision of comparative models with YASARA NOVA-a self-parameterizing force field. Proteins 47(3):393–402.

Kumar V, Yedavalli P, Gupta V, Rao NM. 2014. Engineering lipase A from mesophilic Bacillus subtilis for activity at low temperatures. Protein Eng Des Sel 27(3):73–82.

Lehmann C, Sibilla F, Maugeri Z, Streit WR, de Maria PD, Martinez R, Schwaneberg U. 2012. Reengineering CelA2 cellulase for hydrolysis in aqueous solutions of deep eutectic solvents and concentrated seawater. Green Chem 14(10):2719–2726.

Liszka MJ, Clark ME, Schneider E, Clark DS. 2012. Nature Versus Nurture: Developing Enzymes That Function Under Extreme Conditions. Annu Rev Chem Biomol Eng Vol 3(3):77–102.

Lou WY, Zong MH, Liu YY, Wang JF. 2006. Efficient enantioselective hydrolysis of D, L-phenylglycine methyl ester catalyzed by immobilized Candida antarctica lipase B in ionic liquid containing systems. J Biotechnol 125(1):64–74.

Luczak J, Hupka J, Thoming J, Jungnickel C. 2008. Self-organization of imidazolium ionic liquids in aqueous solution. Colloids and Surfaces A 329(3):125–133.

Mao GX, Zhu AF. 2013. The Aggregation Behavior of Short Chain Hydrophilic Ionic Liquids in Aqueous Solutions. Iran J Chem Chem Eng Int English Ed 32(1):77–82.

Miskolczy Z, Sebok-Nagy K, Biczok L, Gokturk S. 2004. Aggregation and micelle formation of ionic liquids in aqueous solution. Chem Phys Lett 400(4-6):296–300.

Modaressi A, Sifaoui H, Mielcarz M, Domanska U, Rogalski M. 2007. Influence of the molecular structure on the aggregation of imidazolium ionic liquids in aqueous solutions. Colloids Surf A 302(1-3):181–185.

Moniruzzaman M, Nakashima K, Kamiya N, Goto M. 2010. Recent advances of enzymatic reactions in ionic liquids. Biochem Eng J 48(3):295–314.
Mora-Pale M, Meli L, Doherty TV, Linhardt RJ, Dordick JS. 2011. Room Temperature Ionic Liquids as Emerging Solvents for the Pretreatment of Lignocellulosic Biomass. Biotechnol Bioeng 108(6):1229–1245.
Nordwald EM, Brunecky R, Himmel ME, Beckham GT, Kaar JL. 2014. Charge Engineering of Cellulases Improves Ionic Liquid Tolerance and Reduces Lignin Inhibition. Biotechnol Bioeng 111(8):1541–1549.
Nordwald EM, Kaar JL. 2013. Stabilization of Enzymes in Ionic Liquids Via Modification of Enzyme Charge. Biotechnol Bioeng 110(9):2352–2360.
Plechkova NV, Seddon KR. 2007. Ionic Liquids: "Designer" Solvents for Green Chemistry. Tundo P, Perosa A, Zecchini F, editors. Methods and Reagents for Green Chemistry: An Introduction. Hoboken, NJ, USA: John Wiley & Sons, Inc. p 103–130.
Raddadi N, Cherif A, Daffonchio D, Fava F. 2013. Halo-alkalitolerant and thermostable cellulases with improved tolerance to ionic liquids and organic solvents from Paenibacillus tarimensis isolated from the Chott El Fejej, Sahara desert, Tunisia. Bioresour Technol 150:121–128.
Reis P, Holmberg K, Watzke H, Leser ME, Miller R. 2009. Lipases at interfaces: A review. Adv Colloid Interface Sci 147-48:237–250.
Remsing RC, Liu Z, Sergeyev I, Moyna G. 2008. Solvation and aggregation of n,n'-dialkylimidazolium ionic liquids: A multinuclear NMR spectroscopy and molecular dynamics simulation study. J Phys Chem B 112(25):7363–7369.
Schmid RD, Verger R. 1998. Lipases: Interfacial enzymes with attractive applications. Angew Chem Int Ed 37(12):1609–1633.
Singh T, Kumar A. 2007. Aggregation behavior of ionic liquids in aqueous solutions: Effect of alkyl chain length, cations, and anions. J Phys Chem B 111(27):7843–7851.
Sintra TE, Ventura SPM, Coutinho JAP. 2014. Superactivity induced by micellar systems as the key for boosting the yield of enzymatic reactions. J Mol Catal B: Enzym 107:140–151.
Stamatis H, Xenakis A, Kolisis FN. 1999. Bioorganic reactions in microemulsions: the case of lipases. Biotechnol Adv 17(4-5):293–318.
Trivedi N, Gupta V, Reddy CRK, Jha B. 2013. Detection of ionic liquid stable cellulase produced by the marine bacterium Pseudoalteromonas sp isolated from brown alga Sargassum polycystum C. Agardh. Bioresour Technol 132:313–319.
Uppenberg J, Hansen MT, Patkarr S, Jones TA. 1994. The Sequence, Crystal-Structure Determination and Refinement of 2 Crystal Forms of Lipase-B from Candida-Antarctica (Vol 2, Pg 293, 1994). Structure 2(5):453–454.
Vaghela NM, Sastry NV, Aswal VK. 2011. Surface active and aggregation behavior of methylimidazolium-based ionic liquids of type [C-n mim] [X], n=4, 6, 8 and [X] = Cl–, Br-, and I- in water. Colloid Polym Sci 289(3):309–322.
van Pouderoyen G, Eggert T, Jaeger KE, Dijkstra BW. 2001. The crystal structure of Bacillus subtilis lipase: A minimal alpha/beta hydrolase fold enzyme. J Mol Biol 309(1):215–226.
van Rantwijk F, Sheldon RA. 2007. Biocatalysis in ionic liquids. Chem Rev 107(6):2757–2785.
Ventura SPM, Santos LDF, Saraiva JA, Coutinho JAP. 2012. Ionic liquids microemulsions: the key to Candida antarctica lipase B superactivity. Green Chem 14(6):1620–1625.
Wang HY, Wang JJ, Zhang SB, Xuan XP. 2008. Structural Effects of Anions and Cations on the Aggregation Behavior of Ionic Liquids in Aqueous Solutions. J Phys Chem B 112(51):16682–16689.
Wang JJ, Wang HY, Zhang SL, Zhang HH, Zhao Y. 2007. Conductivities, volumes, fluorescence, and aggregation behavior of ionic liquids [C(4) mim][BF4] and [C(n) mim]Br(n = 4, 6, 8, 10, 12) in aqueous solutions. J Phys Chem B 111(22):6181–6188.
Wang WY, Malcolm BA. 1999. Two-stage PCR protocol allowing introduction of multiple mutations, deletions and insertions using QuikChange (TM) site-directed mutagenesis. Biotechniques 26(4):680–682.
Wolski PW, Clark DS, Blanch HW. 2011. Green fluorescent protein as a screen for enzymatic activity in ionic liquid-aqueous systems for in situ hydrolysis of lignocellulose. Green Chem 13(11):3107–3110.
Yang Z, Zhang KP, Huang Y, Wang Z. 2010. Both hydrolytic and transesterification activities of Penicillium expansum lipase are significantly enhanced in ionic liquid [BMIm][PF6]. J Mol Catal B Enzym 63(1-2):23–30.
Zhao H. 2010. Methods for stabilizing and activating enzymes in ionic liquids - a review. J Chem Technol Biotechnol 85(7):891–907.
Zhao J, Kardashliev T, Ruff AJ, Bocola M, Schwaneberg U. 2014. Lessons From Diversity of Directed Evolution Experiments by an Analysis of 3,000 Mutations. Biotechnol Bioeng 111(12):2380–2389.

Supporting Information

Additional supporting information may be found in the online version of this article at the publisher's web-site.